



ELSEVIER

Fusion Engineering and Design 00 (2002) 1–6

**Fusion
Engineering
and Design**

www.elsevier.com/locate/fusengdes

Control of the heavy-ion beam line gas pressure and density in the HYLIFE thick-liquid chamber

Christophe S. Debonnel*, Grant T. Fukuda, Philippe M. Bardet, Per F. Peterson

Department of Nuclear Engineering, University of California at Berkeley, 4118 Etcheverry Hall, Berkeley, CA 94720, USA

Abstract

Controlling the density and pressure of the background gas in the beam lines of thick-liquid heavy-ion fusion chambers is of paramount importance for the beams to focus and propagate properly. Additionally, transport and deposition of debris material onto metal beam-tube surfaces may reduce the breakdown voltage and permit arcing with the beam. The strategy to control the gas pressure and the rate of debris deposition is twofold. First, the cool thick-liquid jet structures will mitigate the venting to the beam tubes. The ablation and venting of debris through thick-liquid structures must be modelled to predict the quantities of debris reaching the beam ports. TSUNAMI calculations have been performed to estimate the mass and energy flux histories at the entrance of the beam ports in a 9×9 HYLIFE pocket geometry. Secondly, additional renewable shielding will be interposed in the beam tubes themselves. Thick-liquid vortexes are planned to coat the inside of the beam tubes and provide a quasi-continuous protection of the beam-tube walls up to the final focus magnets. A three-component molten salt, flinabe, with a low melting temperature and vapor pressure, has been identified as a candidate liquid for the vortexes. The use of flinabe may actually eliminate the necessity of mechanical shutters to rapidly close the beam tubes after target ignition. © 2002 Published by Elsevier Science B.V.

Keywords: Heavy-ion; Gas pressure; Chamber

1. Introduction

Keeping the pressure and density low in the final-focus magnet region of heavy-ion fusion beam lines is very important for the beams to propagate and focus properly. Any stripping of ions by collisions with background gas, prior to or

in the final focus magnet region, causes the ions to be lost. Beyond the final focus magnets, the gas density can climb to the chamber value, but the density distribution and preionization of the gas must be controlled to optimize the beam neutralization and focusing performance. Estimates of the mass flux, pressure and temperature of the debris at the entrance of the beam tubes provide the inlet boundary conditions to determine the amount of debris that must be managed in the beam tubes and diverted from depositing in the final-focus magnet region. Assessments of ablation

* Corresponding author. Tel.: +1-510-642-0421; fax: +1-510-643-9685

E-mail address: debonnel@nuc.berkeley.edu (C.S. Debonnel).

and venting phenomena have been given by Chen [1], Liu [2], Scott [3] and Jantzen [4], but recent improvements in the liquid pocket design require a new investigation to evaluate how effectively the current hybrid HYLIFE II design protects the beam tubes and ultimately the final focus magnets. A detailed assessment of the gas dynamics in a beam tube has never been done before and an outline of the relevant physics is given here, along with the required improvements in numerical modelling that should be made to assess the venting through the beam tubes. Calculations are also presented for the impulse loads delivered to target facing surfaces by X-ray ablation and pocket pressurization, since these loads are important in assessing the liquid response and the effectiveness of pocket regeneration.

2. The target chamber

2.1. Numerical modelling of the target chamber

The Berkeley CFD TSUNAMI code (Chen et al. [5]) has been revised and extended to model the hybrid HYLIFE chamber (Debonnel et al. [6]). It solves the one-dimensional Euler's equations for compressible flow using the Godunov's method as refined by Colella et al. (see [6] and the references therein). Operator splitting is used for two-dimensional calculations.

The fusion pellet and holhraum are modelled as a spherical source emitting a specified amount of debris and a given yield. The target is assumed to radiate X-rays at a single blackbody temperature. The fraction of energy that goes into the X-rays and the one that goes into the debris are specified. The amount of ablated pocket material is assessed via the cohesive energy model. The X-ray energy deposited in target-facing liquid surfaces is computed using photon absorption cross sections, and vaporization is assumed to occur down to the depth where the energy density reaches the cohesive energy. The vaporization is assumed to be instantaneous and is imposed as an initial condition for the subsequent gas dynamics.

Due to their large inertia, the liquid structures are assumed to remain stationary during the entire

venting process. During a TSUNAMI calculation, the liquid jets do not have the time to move notably and the disruption of the jets due to neutron isochoric heating or pressure build-up also happen sufficiently slowly that it does not alter the vent paths geometry, except where the venting gaps are very small. Boundary conditions are open at the location of the beam tubes and the condensing area. (The injected droplets are assumed to condense all of the mass that flows onto them.) The boundary condition is closed at the surface of the thick-liquid structures. Convective transport is assumed to predominate over heat transfer effects at these boundaries. Most of the condensation is expected to occur on droplets in the condensing region.

2.2. Study cases

This analysis considers a two-sided illumination by a 9×9 square beam array. Not all of the positions in the 9×9 lattice are necessarily filled with actual beams. In particular, corner apertures, and likely center ones, are left empty to create a more cylindrically symmetric beam pattern. The 9×9 pocket geometry has been idealized (see Fig. 1), so that it can be modelled with a two-dimensional code. The hybrid target chamber has been assumed to be axially symmetric around the direction of the target injection path.

A real gas equation of state adapted from Chen's work [1] has been employed. The target is assumed to be a sphere of 10 g with a typical yield of 450 MJ, 4% of which is given to the debris, 25% to the X-rays, and the remainder removed by neutrons.

At the very beginning, the vapor in the chamber is quiescent with a pressure corresponding to the saturation one in equilibrium with the liquid at 873 K, where its density is equal to $1.6 \times 10^{-7} \text{ kg m}^{-3}$, as prescribed by Olander et al. [7]. While the equilibrium vapor is composed primarily of the more volatile component BeF_2 , in these TSUNAMI calculations, the gas is assumed to have the same stoichiometric composition as flibe, and mass transfer effects are neglected. This assumption is reasonable because the mass of the initial equilibrium vapor is small compared to the mass

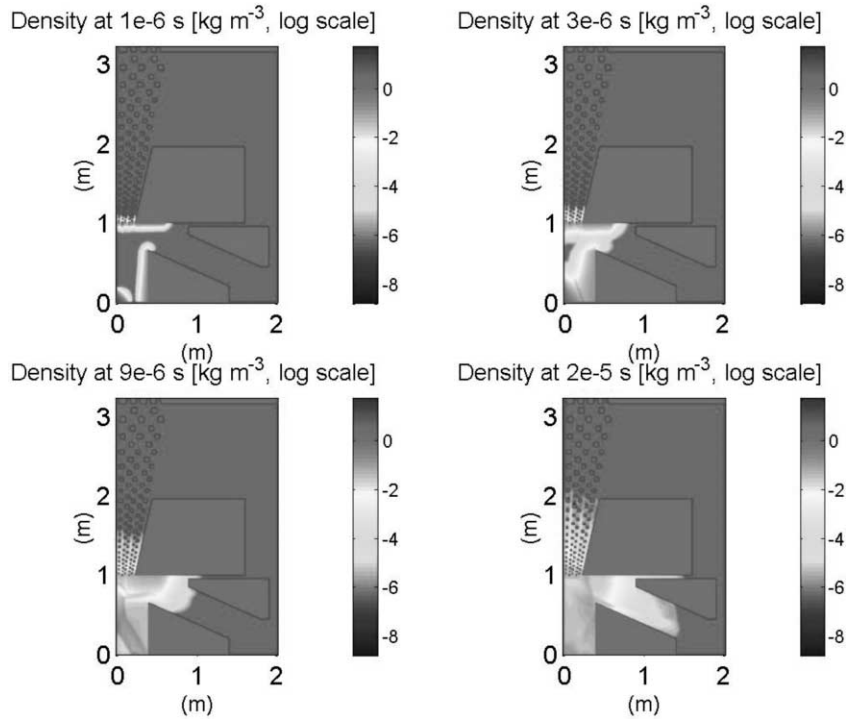


Fig. 1. Density contour plots at various times. The density of the liquid and solid structures is arbitrarily low.

of ablation debris. However, at long times (after a few tens of milliseconds), as the chamber vapor approaches equilibrium conditions before the next shot, LiF and NaF will condense preferentially, modifying the composition in the vapor phase.

2.3. Results

The X-rays vaporize 0.56 kg of flibe. For the standard 9×9 axially symmetric hybrid case (Fig. 1), an integrated mass flux of 1.8 g m^{-2} has been computed after 1 ms at the entrance of a beam tube on the target injection axis (Fig. 2). (In other words, $14 \text{ } \mu\text{g}$ of debris enters the centerline tube per shot.) The integrated energy flux after 1 ms is 3.2 MJ m^{-2} (Fig. 3). (This corresponds to 25 kJ entering the centerline tube per shot.) Off-axis, mass and energy fluxes drop. These two-dimensional TSUNAMI calculations predict a reduction by two orders of magnitude for the fluxes at the entrance of the most off-axis tubes. These results were obtained for a condensing area of 79 m^2 and

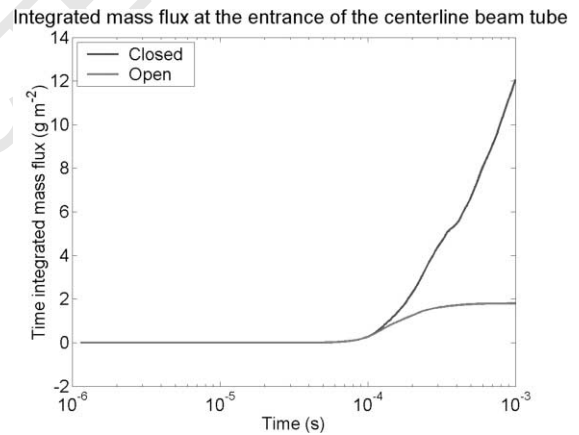


Fig. 2. Integrated mass flux.

are dependent on the area of the chamber wall that is assumed to open into condensing regions. If the chamber wall has no condenser opening, the integrated mass flux rises to 8.0 g m^{-2} in 1 ms and the integrated energy flux is 12 MJ m^{-2} .

Integrated energy flux at the entrance of the centerline beam tube

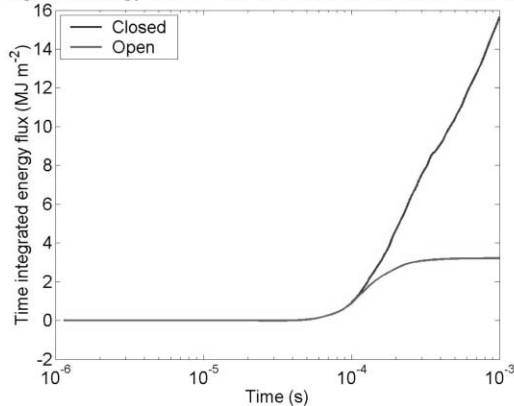


Fig. 3. Integrated energy flux.

The impulse load to the target-facing liquid structures is estimated to be 1.4 kPa s^{-1} (Fig. 4). The first rise is due to the expansion of the ablation debris, which exercise pressure work on the jets. The pocket pressurization causes the second rise in impulse load. Numerical convergence has been investigated by decreasing the Courant–Friedrichs–Lewy (CFL) number and the mesh size. With a smaller CFL number, the tracking of the shock waves is improved but the results are similar. Decreasing the size of the mesh did not change the results significantly.

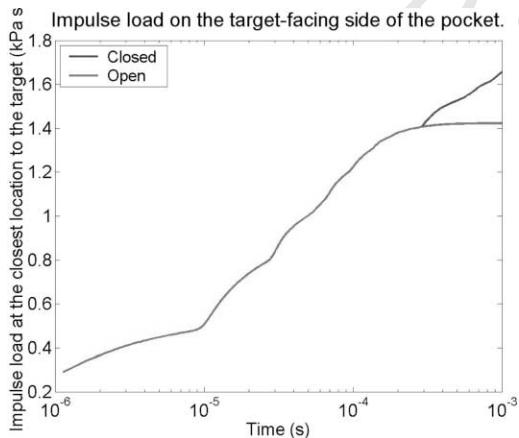


Fig. 4. Impulse load.

3. The beam tubes

173

3.1. Flibe versus flinabe

174

Controlling the pressure in the beam tube requires the careful choice of the thick liquid composition used and its temperature. Neutronics and the effectiveness of magnet shielding, as well as thermal hydraulics properties must be taken into account. The blanket must also breed the tritium fuel required by traditional DT targets. HYLIFE I was designed to use liquid lithium. HYLIFE II uses the molten salt flibe instead, to decrease the fire hazard and improve neutron shielding effectiveness, while preserving tritium breeding and good neutronics properties. However, the melting temperature and vapor pressure of flibe are a concern. An approach to reducing the melting temperature of flibe substantially has been identified. Some of the lithium fluoride (LiF) may be replaced by sodium fluoride (NaF).

Adding roughly 30% NaF to flibe, creating “flinabe”, depresses the melting temperature from 733 K to less than 673 K. When used at temperatures below the melting temperature of flibe, this ternary salt mixture has a much lower equilibrium vapor pressure (roughly estimated to be 0.1 mPa at 713 K) and density (around 10^{16} m^{-3}), which makes it compatible for use in heavy-ion beam lines. Adding up to 25% NaF is not expected to decrease the breeding factor enough to cause concern, as estimated by Latkowski [8]. Flinabe might therefore be used instead of flibe in the target chamber as well as in the beam tubes, simplifying the overall hydraulics design by having one coolant loop instead of two.

3.2. Flinabe: the panacea?

207

As shown in Fig. 5, one or two vortices would be used. Such vortices have been demonstrated to be feasible in scaled water experiments [9]. One vortex would coat the inside of the beam tube up to the neutralization area, and possibly a second vortex would extend from there through the final focus magnet region. The vapor pressure of flinabe is sufficiently low that it can be used to cover the inside of the beam tubes in the final focus magnets

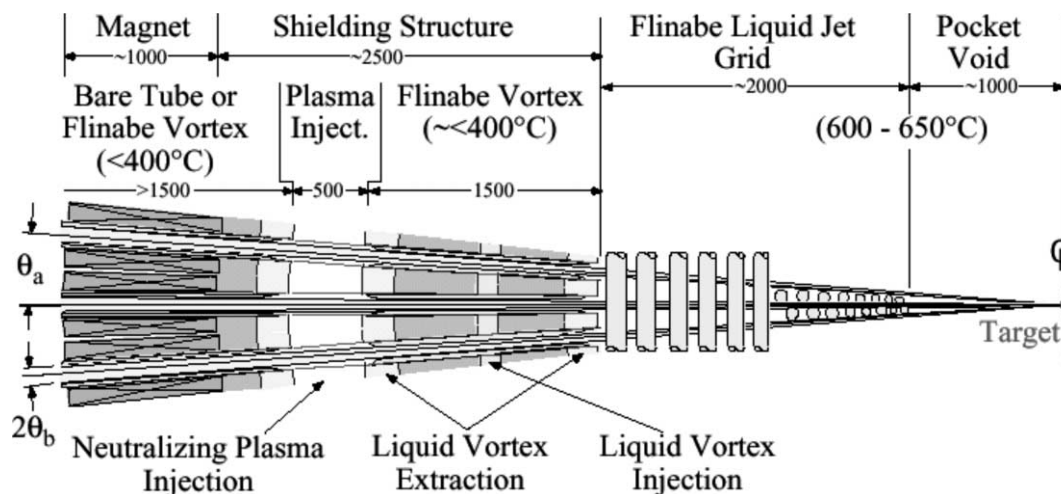


Fig. 5. Beam-line schematic. Lengths are in mm. θ_a is the array half-angle, θ_b the beam half-angle.

region. An effective coating of the beam tubes may alleviate the burden of using shutters to protect the beam tubes.

However, the electrical breakdown properties of flinabe liquid surfaces remain to be investigated. A high resistivity may induce an electrical breakdown during the passage of the beams upstream of the neutralization point, where the high space charge of the beams creates high electrical fields. For an unneutralized 4-kA beam, moving at 20% of the speed of light, and a pipe radius of 5 cm, the steady electric field is 200 kV cm^{-1} . This is substantially more than the 20 kV cm^{-1} typically required to generate voltage breakdown with insulators. However the liquid flinabe will likely have different characteristics than solid insulators. In particular flinabe will have much lower absorbed gas concentrations than typical solid insulators: Absorbed gas is actually believed to generate the initial electrons required for surface breakdown and flashover in most insulators. The short duration of a beam pulse may help to alleviate this flashover concern too.

3.3. Qualitative gas dynamics in the beam tubes

The first puffs of ablation debris will be hot enough to vaporize some flinabe from the surface of the beam tube vortex. Along the beam tubes, the gas will cool by heat transfer and by mixing

with evaporated vortex liquid, and ultimately will condense. An efficient thick-liquid protection scheme should cause all the ablation debris to condense before the final-focus region or would otherwise prevent the gas from reaching the final-focus magnet region.

A detailed assessment of the mass flux at the entrance of the beam lines will require the consideration of three-dimensional effects, as well as a refined real gas equation of state and treatment of evaporation and condensation on liquid surfaces in the jet array. The current code and computing power do not allow the concurrent simulation of the target chamber and beam tubes. Runs for the beam tubes will have to be performed separately, using the results from target chambers simulations as inlet conditions. Therefore, a time-dependent boundary condition capability will have to be implemented into TSUNAMI.

4. Conclusion

Mass and energy fluxes at the entrance of the centerline beam tube have been estimated. The chamber volume and condenser area are key components in controlling the mass flux at the entrance of the beam tubes, since it determines how rapidly the average gas pressure drops in the chamber. The hot puff that originally enters the

272 beam tubes is expected to vaporize some of the
273 vortex liquid, whereas condensation should be a
274 key process to keep the pressure and density low
275 further up in the beam tubes.

276 Acknowledgements

277 This work was performed under the auspices of
278 the US Office of Fusion Energy Science under
279 contract DE-FG03-97ER5441. Fruitful conversa-
280 tions with Dr Yu from LBNL are gratefully
281 acknowledged.

282 References

- 283 [1] X.M. Chen, A Study of Thermal Hydraulic and Kinetic
284 Phenomena in HYLIFE-II—An Inertial Confinement Fu-
285 sion Reactor, Ph.D. thesis, University of California at
286 Berkeley, 1992.
310

- [2] J.C. Liu, Experimental and Numerical Investigation of
Shock Wave Propagation Through Complex Geometry,
Gas Continuous, Two-Phase Media, Ph.D. thesis, Univer-
sity of California at Berkeley, 1993.
[3] J.M. Scott, X-Ray Ablated Plumes in Inertial Confinement
Fusion Reactors, Ph.D. thesis, University of California at
Berkeley, 1998.
[4] C.A. Jantzen, Gas Dynamics and Radiative Heat Transfer
in IFE Chambers with Emphasis on the HYLIFE-II Design,
Ph.D. thesis, University of California at Berkeley, 2000.
[5] X.M. Chen et al., Code Description Document, TSUNAMI
2.6: A Program for Predicting Gas Dynamics in Inertial
Fusion Energy Target Chambers, Nuclear Engineering
Department, University of California at Berkeley, 1998.
[6] C.S. Debonnel et al., Code Description for TSUNAMI
2.8.2, personal document, 2002.
[7] D.R. Olander, G. Fukuda, C.F. Baes, Equilibrium pressures
over BeF₂/LiF (flibe) molten mixtures, Fusion Science and
Technology 41–2 (2002) 141–150.
[8] J.F. Latkowski, personal communication, 2001.
[9] S.J. Pemberton, Thick Liquid Protection in Inertial Fusion
Power Plants, Ph.D. thesis, University of California at
Berkeley, 2002.